Monthly Notices of the ROYAL ASTRONOMICAL SOCIETY

MNRAS **529,** 831–838 (2024) https://doi.org/10.1093/mnras/stae402
Advance Access publication 2024 February 27

Exploring modified gravity: constraints on the μ and Σ parametrization with *WMAP*, ACT, and SPT

Uendert Andrade [1,2,3★] Abraão J. S. Capistrano [4,5★] Eleonora Di Valentino [6★] and Rafael C. Nunes [7,8★]

[1]*Leinweber Center for Theoretical Physics, University of Michigan, 450 Church Street, Ann Arbor, MI 48109-1040, USA*
[2]*Department of Physics, College of Literature, Science and the Arts, University of Michigan, 450 Church Street, Ann Arbor, MI 48109-1040, USA*
[3]*Observatório Nacional, Rio de Janeiro 20921-400, RJ, Brazil*
[4]*Departamento de Engenharias e Exatas, Universidade Federal do Paraná, Palotina 85950-000, PR, Brazil*
[5]*Applied Physics Graduation Program, UNILA, Foz do Iguaçu 85867-670, PR, Brazil*
[6]*School of Mathematics and Statistics, University of Sheffield, Hounsfield Road S3 7RH Sheffield United Kingdom*
[7]*Instituto de Física, Universidade Federal do Rio Grande do Sul, Porto Alegre 91501-970, RS, Brazil*
[8]*Divisão de Astrofísica, Instituto Nacional de Pesquisas Espaciais, Avenida dos Astronautas 1758, São José dos Campos 12227-010, SP, Brazil*

Accepted 2024 January 29. Received 2023 December 22; in original form 2023 October 5

ABSTRACT

The cosmic acceleration problem remains one of the most significant challenges in cosmology. One of the proposed solutions to this problem is the modification of gravity on large scales. In this paper, we explore the well-known μ–Σ parametrization scenarios and confront them with observational data, including the cosmic microwave background (CMB) radiation from the *Wilkinson Microwave Anisotropy Probe* (*WMAP*), Atacama Cosmology Telescope (ACT), and South Pole Telescope (SPT), as well as large-scale structure data from the Sloan Digital Sky Survey (SDSS; baryon acoustic oscillation + redshift-space distortion) and Pantheon supernova (SN) catalogue. We employ a Bayesian framework to constrain the model parameters and discuss the implications of our results on the viability of modified gravity theories. Our analysis reveals the strengths and limitations of the μ–Σ parametrization and provides valuable insights into the nature of gravity on cosmological scales. From the joint analysis of the ACT + *WMAP* + SDSS + SN, we find $\mu_0 - 1 = 0.02 \pm 0.19$ and $\Sigma_0 - 1 = 0.021 \pm 0.068$ at 68 per cent confidence level (CL). In light of the SPT + *WMAP* + SDSS + SN, we find $\mu_0 - 1 = 0.07 \pm 0.18$ and $\Sigma_0 - 1 = -0.009^{+0.078}_{-0.11}$ at 68 per cent CL. In all the analyses carried out, we do not find any deviations from the theory of general relativity. Our results represent an observational update on the well-known μ–Σ parametrization in view of current CMB data, independent of and competitive with the constraints obtained with the *Planck* data.

Key words: cosmic background radiation – cosmological parameters – dark energy.

1 INTRODUCTION

The standard cosmological model, based on the framework of general relativity (GR) and the presence of dark energy in the form of a cosmological constant (Λ), has been remarkably successful in explaining a wide range of observations, including the cosmic microwave background (CMB) anisotropies (Bennett et al. 2013; Aiola et al. 2020; Planck Collaboration VI 2020a; Balkenhol et al. 2023), large-scale structure (LSS; Abazajian et al. 2009; Song & Percival 2009; Davis et al. 2011; Beutler et al. 2012; Blake et al. 2012; Tojeiro et al. 2012; Sánchez et al. 2014; Huterer et al. 2017; Zarrouk et al. 2018; Alam et al. 2021), and Type Ia supernovae (SNeIa; Scolnic et al. 2018; Brout et al. 2022), among several other observations at both astrophysical and cosmological scales (Asgari et al. 2021; Amon et al. 2022; Abbott et al. 2023a, b; Dalal et al. 2023; Li et al. 2023). However, despite its successes, the standard model faces several challenges. One of the most significant problems is the so-called cosmic acceleration problem. Observations of distant SNe (Riess et al. 1998; Perlmutter et al. 1999) have shown that the Universe is currently undergoing an accelerated expansion, implying the existence of a mysterious form of energy with negative pressure, often referred to as dark energy. Although a cosmological constant is a simple and viable candidate for dark energy, its small but non-zero value, when compared to theoretical predictions, has led to the so-called fine-tuning problem and the coincidence problem (Weinberg 1989; Zlatev, Wang & Steinhardt 1999; Padmanabhan 2003; Velten, vom Marttens & Zimdahl 2014).

An alternative approach to explaining cosmic acceleration is to modify the laws of gravity on cosmological scales. The modified gravity (MG) scenarios may allow for extensions of the Lambda cold dark matter (ΛCDM) model, which exhibit the accelerated expansion of the Universe at late times, as well as explain various observations at the cosmological and astrophysical levels. See Ishak (2019), Heisenberg (2019), Akrami et al. (2021), and Nojiri, Odintsov & Oikonomou (2017) for a recent review. On the other hand, still from an observational point of view, some recent tensions and anomalies

★ E-mail: uendsa@umich.edu (UA); abecapistrano@gmail.com (AJSC); e.divalentino@sheffield.ac.uk (EDV); rafadcnunes@gmail.com (RCN)

have turned out to be statistically significant, while analysing different data sets. The most long-lasting disagreement is in the value of the Hubble constant, H_0, between the CMB, estimated assuming the standard ΛCDM model (Planck Collaboration VI 2020a), and the direct local distance ladder measurements, conducted by the SH0ES team (Riess et al. 2022, 2023), reaching a significance of more than 5σ. Further, within the ΛCDM framework, the CMB measurements from *Planck* and Atacama Cosmology Telescope (ACT; Aiola et al. 2020; Planck Collaboration VI 2020a; Qu et al. 2023) provide values of $S_8 = \sigma_8\sqrt{\Omega_{\rm m}/0.3}$ in 1.7–3σ statistical tension with the ones inferred from various weak lensing, galaxy clustering, and redshift-space distortion (RSD) measurements (Asgari et al. 2021; Di Valentino et al. 2021b; Nunes & Vagnozzi 2021; Amon et al. 2022; Abbott et al. 2023a, b; Dalal et al. 2023; Li et al. 2023). Various other anomalies and tensions have been emerging within the ΛCDM framework in the recent years (Abdalla et al. 2022; Perivolaropoulos & Skara 2022). Motivated by such discrepancies, it has been widely discussed in the literature whether new physics beyond the standard cosmological model may solve these tensions, and theories beyond GR may serve as alternative routes to explain these current tensions (Di Valentino et al. 2021a; Abdalla et al. 2022).

Interestingly, another avenue for probing the nature of cosmic acceleration involves agnostic or empirical tests of gravity theories. For instance, a recent study focused on a general test of the ΛCDM and ωCDM[1] cosmological models by comparing constraints on the geometry of the expansion history to those on the growth of structure, offering a model-independent way to constrain deviations from the standard model (Andrade et al. 2021). This empirical approach provides a complementary methodology to the model-based investigations, potentially revealing new insights into the nature of gravity and dark energy. Other model-independent proposals also explore this possibility performing constraints on possible deviations of gravity, such as (μ–γ) parametrization by Cepheids, tip of red giant branch stars, and water masers (Jain, Vikram & Sakstein 2013), and on ultralarge scales (Baker & Bull 2015), forecasts of growth rate data for *Euclid* and Square Kilometre Array (SKA) surveys (Taddei, Martinelli & Amendola 2016), constraints on $f(T)$ gravity models (Nunes, Pan & Saridakis 2016) using cosmic chronometers (CC; Moresco 2015) with a combination of SNIa + baryon acoustic oscillation (BAO) data and galaxy clusters + BAO + CMB + CC + Pantheon (dos Santos, Gonzalez & Silva 2022), and N-body simulations of MG gravity (Thomas 2020; Srinivasan et al. 2021) have been tested.

In this work, we focus on updating observational constraints on the popular (μ–Σ) MG functions, which wrap up the Horndeski class of scalar–tensor theories (Horndeski 1974; Deffayet et al. 2011). The Horndeski theories of gravity are the most general Lorentz invariant scalar–tensor theories with second-order equations of motion and where all matter is universally coupled to gravity. The Horndeski gravity includes as a subset several archetypal modifications of gravity. See Kase & Tsujikawa (2019) and Kobayashi (2019) for a recent review and the observational status in the Horndeski gravity framework. For this purpose, we confront parametric classes of MG functions with a combination of observational data sets, including CMB data from *Wilkinson Microwave Anisotropy Probe* (*WMAP*), ACT, and South Pole Telescope (SPT), as well as LSS data from Sloan Digital Sky Survey (SDSS)–BAO samples and the Pantheon SNIa catalogue. We consider alternative CMB data to *Planck*, because this is affected by the $A_{\rm lens}$ problem, and it is possibly biasing the results in favour of MG at 2σ level (Di Valentino, Melchiorri & Silk 2016a; Planck Collaboration XIV 2016; Planck Collaboration VI). We employ a Bayesian framework to infer the model parameters from the data and investigate the implications of our findings for the feasibility of an MG dynamics framework during late times.

The structure of the paper is as follows: In Section 2, we present a brief overview of the parametrized MG functions adopted in this work. In Section 3, we describe the observational data sets used in our analysis. In Section 4, we present our Bayesian data analysis framework and discuss the results. Finally, in Section 5, we summarize our findings and provide concluding remarks. As usual, a sub-index zero attached to any quantity means that it must be evaluated at the present time.

2 ESSENTIALS ON (μ–Σ) PARAMETRIZATION

In essence, MG functions μ, Σ, and η are designed to parametrize potential deviations from GR by comparing the Bardeen potentials: specifically, the curvature perturbation Φ and the Newtonian potential Ψ. These parameters form a framework that encapsulates deviations from GR through two phenomenological functions: the effective gravitational coupling μ and the light deflection parameter Σ. Here, μ quantifies how gravitational interactions that cluster matter diverge from the standard ΛCDM model, while Σ assesses variations in the lensing gravitational potential. Additionally, a third MG function, η, known as the gravitational slip parameter, can be introduced as a combination of the first two.

The starting point is to consider the perturbed Robertson–Walker metric in conformal Newtonian gauge,

$$ds^2 = a(\tau)^2\left[-(1+2\Psi)d\tau^2 + (1-2\Phi)\gamma_{ij}dx^i dx^j\right], \quad (1)$$

where τ is conformal time, $a = 1/(1+z)$ is the expansion scale factor, and γ_{ij} is the 3-metric for a space of constant spatial curvature K. We neglect entropy perturbations and consider only curvature perturbations on a flat ($K = 0$) background.

MG theories impact the linear evolution of cosmological perturbations by modifying the Poisson and anisotropic stress equations, i.e.

$$k^2\,\Psi(a,k) = -\frac{4\pi G}{c^4}\mu(a,k)\,a^2\,\bar{\rho}\Delta, \quad (2)$$

$$\Phi(a,k) = \Psi(a,k)\,\eta(a,k), \quad (3)$$

$$k^2\,[\Phi(a,k)+\Psi(a,k)] = -\frac{8\pi G}{c^4}\Sigma(a,k)\,a^2\,\bar{\rho}\Delta, \quad (4)$$

where $\bar{\rho}\Delta = \bar{\rho}\delta + 3(aH/k)(\bar{\rho}+\bar{p})v$ is the comoving density perturbation of $\delta = (\rho-\bar{\rho})/\bar{\rho}$, and ρ, p, and v are, respectively, the density, pressure, and velocity with the bar sign denoting mean quantities. The MG functions μ and η enter the Poisson equation (2) and the potentials relation by equation (3), whereas Σ enters the lensing equation (4), respectively. Of the three functions, only two are independent, and the system of the free functions (2), (3), and (4) reduces to the closure relation

$$\Sigma(a,k) = \frac{\mu(a,k)}{2}\,(1+\eta(a,k))\,. \quad (5)$$

From the former equation (5), it is worth noting that the ΛCDM model is recovered when $\mu = \eta = \Sigma = 1$.

In a ΛCDM framework and minimally coupled dark energy models, the anisotropic stress is negligible at times relevant for

[1]The ωCDM model is an extension of the ΛCDM model that allows the equation of state of dark energy to deviate from the constant value of −1, usually parametrized by a constant ω. See Escamilla et al. (2023) for a recent work.

structure formation, and we have $\Phi = \Psi$. This methodology has been used to investigate efficiently the most diverse proposals of MG scenarios (see Zhao et al. 2009, 2010; Giannantonio et al. 2010; Pogosian et al. 2010; Di Valentino, Melchiorri & Silk ; Salvatelli, Piazza & Marinoni 2016; Espejo et al. 2019; Lin, Raveri & Hu 2019; Frusciante 2021; Sakr & Martinelli 2022; Abbott et al. 2023b; Kumar, Nunes & Yadav 2023; Raveri et al. 2023; Specogna et al. 2023 for a short list). This framework has been recently interpreted in light of H_0, S_8, and the A_L tensions (Pogosian et al. 2022).

In addition to the effects of MG, the evolution of all cosmological perturbations depends on the background expansion. We restrict ourselves to background histories consistent with the flat ΛCDM model. To arrive at a suitable parametrization of the functions μ and Σ, we note that such MG models typically introduce a transition scale that separates regimes where gravity behaves differently. One of the most commonly used parametrizations expresses the MG functions in a way that is typical of theories encompassed in the Horndeski class, i.e.

$$\mu(k,a) = 1 + f_1(a)\frac{1 + c_1\left(\frac{\mathcal{H}}{k^2}\right)}{1 + \left(\frac{\mathcal{H}}{k^2}\right)}, \tag{6}$$

$$\eta(k,a) = 1 + f_2(a)\frac{1 + c_2\left(\frac{\mathcal{H}}{k^2}\right)}{1 + \left(\frac{\mathcal{H}}{k^2}\right)}. \tag{7}$$

In the above equations, $\mathcal{H}$ is the comoving Hubble parameter. Such a parametrization has been widely used by *Planck* (Planck Collaboration XIV 2016; Planck Collaboration VI 2020a) and Dark Energy Survey (DES) (Abbott et al. 2019, 2023b) collaborations to constrain possible deviations from GR. For derivation of these equations, see Planck Collaboration XIV (2016) and references therein. The functions $f_i(a)$ regulate the amplitude, in redshift, of such deviations, while the c_i parameters affect their scale dependence. Given that, we expect the MG functions to reduce to their GR limit at early times, as the modifications to the theory of gravity should be relevant only at late times, it is common to assume that the amplitude of the modifications scales with the dark energy density $\Omega_{\rm DE}(a)$ (Planck Collaboration XIV 2016) in such a form

$$f_i(a) = E_{ii}\Omega_{\rm DE}(a). \tag{8}$$

When using these parametrizations throughout the paper, we set ourselves in the scale-independent limit, where $c_1 = c_2 = 1$. This is motivated by the fact that we will mainly use CMB data to constrain such parametrizations, and it has been found that these do not allow to constrain the scale dependence of these MG models (Planck Collaboration XIV 2016). Then, we first adopt the (μ–η) parametrization model as

$$\mu(a) = 1 + E_{11}\Omega_{\rm DE}(a), \tag{9}$$

$$\eta(a) = 1 + E_{22}\Omega_{\rm DE}(a), \tag{10}$$

to find the third MG function Σ that is defined from equation (5). Therefore, our free parameter that quantifies possible deviations from GR will be determined by the values of the parameters E_{11} and E_{22}. When $E_{11} = E_{22} = 0$, we recover GR.

It is crucial to emphasize that our outlined approach remains valid and well behaved within the sub-horizon and quasi-static regimes. However, for scales extending beyond the quasi-static regime and perturbation modes approaching the Hubble scale, as discussed in previous works of Baker & Bull (2015) and Baker et al. (2014), the functional and parametric forms of equations (6)–(10) should be scale dependent. Moreover, they should account for the existence of a time-scale characterizing deviations from GR. In practice, such corrections and parametrizations need meticulous consideration, particularly when applied to full-sky CMB data, such as *WMAP* and *Planck* data. Consequently, we assert that our analysis and primary findings in this work should be interpreted optimistically. The parametrization presented can be viewed as an empirical model that, in principle, remains independent of underlying theories.

3 METHODOLOGY AND DATA SET

In our analysis, we consider a range of observational data from various sources that provide complementary and independent cosmology probes, including CMB measurements, LSS distributions, and SNeIa. In what follows, we define our data sets.

3.1 CMB data

For the CMB data, we use the power spectrum data from temperature and polarization maps of the *WMAP*, the ACT, and the SPT. The *WMAP* mission has comprehensively assessed CMB radiation's temperature, polarization, and lensing maps across the entire sky. We utilize the data from the 9 yr *WMAP* temperature, polarization, and lensing maps (Bennett et al. 2013). However, we chose to exclude the TE data at low ℓ, setting the minimum multipole in TE at $\ell = 24$, considering our utilization of a Gaussian prior $\tau = 0.065 \pm 0.0015$. The ACT and SPT are ground-based telescopes located in the Atacama Desert of Chile and the South Pole, respectively. They offer high-resolution CMB measurements, complementing the *WMAP* data. We incorporate the latest publicly available data sets from ACT DR4 TTTEEE (Aiola et al. 2020; Choi et al. 2020) combined with ACT DR6 lensing (Madhavacheril et al. 2023; Qu et al. 2023) and SPT-3G 2018 TT/TE/EE (Balkenhol et al. 2023).

3.2 Large-scale structure data

LSS data provide crucial observational constraints, particularly on the growth of structure, which is sensitive to potential modifications of gravity. We employ the BAO data primarily from the SDSS. BAO represents a regular, periodic fluctuation in the density of the visible baryonic matter in the Universe. This feature provides a 'standard ruler' for determining cosmological length-scales. Besides BAO, the SDSS offers insights into RSDs. These RSDs arise due to the peculiar velocities of galaxies, causing an anisotropic distribution of galaxies in redshift space compared to real space. They capture the growth rate of cosmic structures through the $f\sigma_8$ parameter.

We consider the Seventh Data Release of SDSS Main Galaxy Sample (SDSS DR7 MGS; Ross et al. 2015) and final clustering measurements (Alam et al. 2021) of the Extended Baryon Oscillation Spectroscopic Survey (eBOSS) associated with the SDSS's Sixteenth Data Release (Alam et al. 2017). This collection encompasses data from luminous red galaxies, emission line galaxies, quasars, the Lyman–alpha forest autocorrelation (*lyauto*), and the Lyman–alpha forest x Quasar cross-correlation (*lyxqso*). Each data set uniquely mirrors distinct facets of the Universe's LSSs. Together, they not only amplify the constraints set by BAO observations but also underscore the significance of the SDSS's $f\sigma_8$ measurements, tracking the growth rate evolution across redshifts.

Specifically, concerning BAO samples, our focus will be on utilizing the geometrical measurements outlined below.

(i) The Hubble distance at redshift z:

$$D_{\rm H}(z) = \frac{c}{H(z)}, \tag{11}$$

where $H(z)$ is the Hubble parameter.

(ii) The comoving angular diameter distance, $D_M(z)$, which also only depends on the expansion history:

$$D_M(z) = \frac{c}{H_0}\int_0^z \mathrm{d}z' \frac{H_0}{H(z')}. \quad (12)$$

(iii) The spherically averaged BAO distance:

$$D_V(z) = r_d[zD_M^2(z)D_H(z)]^{1/3}, \quad (13)$$

where r_d is the BAO scale, of which in our analyses we treat it as a derived parameter.

For the growth measurements, the growth function f can be expressed as a differential in the amplitude of linear matter fluctuations on a comoving scale of 8 h^{-1} Mpc, $\sigma_8(z)$, in the form

$$f(z) = \frac{\partial \ln \sigma_8}{\partial \ln a}. \quad (14)$$

The RSD measurements provide constraints on the quantity $f(z)\sigma_8(z)$. The $\sigma_8(z)$ depends on the matter power spectrum, $P(k, z)$, which is calculated by default in the Boltzmann code. Both $f(z)$ and $\sigma_8(z)$ are sensitive to variations in the effective gravitational coupling and the light deflection parameter, which play a crucial role in our Poisson and lensing equations. The cosmological parameters are determined by minimizing the likelihood, as described in section 3.6 of Alam et al. (2021). Our compilation of BAO + RSD results is summarized in table 3 of the same reference.

The precision of these data sets, combined with their broad coverage of various cosmic structures, makes them invaluable in probing cosmological parameters. The BAO and RSD measurements from SDSS, in particular, have been pivotal in constraining the nature of dark energy, the curvature of the Universe, and potential modifications to the standard model of cosmology. In what follows, we refer to these combined data sets, BAO + RSD, simply as SDSS.

Therefore, the BAO scale serves as an important complementary probe to other cosmological observables. When combined with data such as the CMB or SNeIa observations, it allows for tighter constraints on the cosmological parameters, revealing potential tensions or discrepancies that could hint at new physics.

3.3 Type Ia supernovae data

We include the Pantheon SNeIa data set to supplement our data, which provides measurements of SN luminosity distances (Scolnic et al. 2018). This data set combines multiple SN surveys to provide a large, homogeneous set of SN observations covering a wide range of redshifts. SNeIa, as 'standard candles', are crucial in the study of the rate of expansion of the Universe.

The cosmological parameters are constrained by minimizing the χ^2 likelihood

$$-2\ln(L) = \chi^2 = \Delta \boldsymbol{D}^T C^{-1}_{\mathrm{stat+syst}} \Delta \boldsymbol{D}, \quad (15)$$

where $\boldsymbol{D}$ is the vector of 1048 SN distance modulus residuals computed as $\Delta \boldsymbol{D}_i = \mu_i - \mu_{\mathrm{model}}(z_i)$, where the model distances are defined as

$$\mu_{\mathrm{model}}(z_i) = 5\log(d_{\mathrm{L}}(z_i)/10\,\mathrm{pc}), \quad (16)$$

where d_{L} is the model-based luminosity distance that includes the parameters describing the background expansion history of the model. In equation (15), the amount $C^{-1}_{\mathrm{stat+syst}}$ is the inverse of the covariance matrix that accounts for statistical and systematic effects in the samples (Scolnic et al. 2018).

Table 1. Cosmological parameters and their respective priors used in the parameter estimation analysis.

Parameter	Prior
$\Omega_{\mathrm{b}}h^2$	$\mathcal{U}[0.017, 0.027]$
$\Omega_{\mathrm{c}}h^2$	$\mathcal{U}[0.09, 0.15]$
θ_{MC}	$\mathcal{U}[0.0103, 0.0105]$
τ_{reio}	$\mathcal{N}[0.065, 0.0015]$
$\log(10^{10}A_{\mathrm{s}})$	$\mathcal{U}[2.6, 3.5]$
n_{s}	$\mathcal{U}[0.9, 1.1]$
E_{11}	$\mathcal{U}[-1, 3]$
E_{22}	$\mathcal{U}[-1.4, 5]$

3.4 Methodology

We perform a Bayesian analysis to infer the parameters of the μ and Σ parametrization using the data from *WMAP*, ACT, SPT, SDSS–BAO, and the Pantheon SN catalogue. The likelihood function is constructed using the standard chi-square statistic for each data set. The likelihoods from different data sets are then multiplied to obtain a combined likelihood function. For such, we use MGCAMB + COBAYA code (Torrado & Lewis 2021; Wang et al. 2023) with Metropolis–Hastings mode to derive constraints on cosmological parameters for our model baseline from several combinations of the data sets defined above, ensuring a Gelman–Rubin convergence criterion of $R - 1 < 0.03$ in all the runs. Systematic uncertainties associated with each data set are taken into account in our analysis. We consider calibration uncertainties, beam uncertainties, and foreground contamination for the CMB data. For the LSS and SN data, we consider uncertainties related to bias correction, RSDs, and observational errors. These systematic uncertainties are incorporated into our likelihood function. We note that our work focuses on the constraints on the μ and Σ parametrization, and we do not consider other cosmological parameters in detail. However, for a comprehensive understanding, we do include the standard six cosmological parameters of the ΛCDM model in our Markov chain Monte Carlo analysis:

(i) Baryon density, $\Omega_{\mathrm{b}}h^2$;
(ii) Cold dark matter density, $\Omega_{\mathrm{c}}h^2$;
(iii) The angular size of the sound horizon at recombination, θ_{MC};
(iv) Scalar spectral index, n_{s};
(v) Amplitude of primordial fluctuations, A_s;
(vi) Reionization optical depth, τ.

The priors for these parameters have been chosen according to the findings of the Planck 2018 release (Planck Collaboration VI 2020a). These priors are listed in Table 1. In the following section, we will present the results of our Bayesian analysis and discuss the implications for MG theories.

4 RESULTS

In this section, we detail the outcomes of our Bayesian analysis that seeks to understand the implications of the current data for MG theories. Our research is firmly rooted in a robust examination of cosmological parameters, supported by the priors outlined in Table 1. In all main results of this work, the observational constraints obtained on E_{11} and E_{22} are converted to obtain derived constraints on the parameters μ_0, η_0, and Σ_0.

We first consider ACT DR4 data without the lensing likelihood. We note that all the MG baseline, i.e. the parameters μ_0, η_0, and Σ_0 are consistent with GR. Specifically, when considering only ACT DR4 data, we find that the constraints on these parameters

Table 2. Summary of 68 per cent CL limits for different data sets. ACT DR4 = ACT DR4 TT/TE/EE.

Parameter	ACT DR4	ACT DR4 + *WMAP*	ACT DR4 + *WMAP* + SDSS	ACT DR4 + *WMAP* + SDSS + SN
$\Omega_b h^2$	$0.021\,53 \pm 0.000\,32$	$0.022\,40 \pm 0.000\,20$	$0.022\,42 \pm 0.000\,18$	$0.022\,43 \pm 0.000\,18$
$\Omega_c h^2$	0.1168 ± 0.0047	0.1191 ± 0.0027	0.1190 ± 0.0013	0.1189 ± 0.0012
θ_{MC}	$0.010\,4232 \pm 0.000\,0076$	$0.010\,4180 \pm 0.000\,0065$	$0.010\,4182 \pm 0.000\,0060$	$0.010\,4182 \pm 0.000\,0059$
τ	0.0650 ± 0.0015	0.0649 ± 0.0015	0.0650 ± 0.0015	0.0651 ± 0.0015
$\log(10^{10}A_s)$	3.048 ± 0.017	3.0703 ± 0.0085	3.0701 ± 0.0055	3.0701 ± 0.0054
n_s	1.011 ± 0.017	0.9745 ± 0.0063	0.9749 ± 0.0041	0.9749 ± 0.0042
E_{11}	<0.0643	$-0.02^{+0.32}_{-0.59}$	0.02 ± 0.28	0.02 ± 0.29
E_{22}	<1.47	$0.52^{+0.75}_{-1.6}$	$0.26^{+0.55}_{-0.91}$	$0.27^{+0.56}_{-0.91}$
H_0	68.3 ± 1.9	68.0 ± 1.2	68.07 ± 0.54	68.09 ± 0.51
σ_8	$0.808^{+0.038}_{-0.048}$	$0.822^{+0.032}_{-0.039}$	0.824 ± 0.021	0.823 ± 0.021
$\mu_0 - 1$	$-0.12^{+0.22}_{-0.53}$	$-0.01^{+0.23}_{-0.40}$	0.02 ± 0.20	0.01 ± 0.20
$\eta_0 - 1$	$0.56^{+0.59}_{-1.4}$	$0.36^{+0.55}_{-1.1}$	$0.18^{+0.38}_{-0.63}$	$0.19^{+0.38}_{-0.63}$
$\Sigma_0 - 1$	$-0.04^{+0.19}_{-0.26}$	$0.056^{+0.082}_{-0.15}$	$0.063^{+0.082}_{-0.15}$	$0.064^{+0.085}_{-0.16}$

Table 3. Summary of 68 per cent CL limits for different data sets. ACT = ACT DR4 TT/TE/EE DR6 lensing.

Parameter	ACT	ACT + *WMAP*	ACT + *WMAP* + SDSS	ACT + *WMAP* + SDSS + SN
$\Omega_b h^2$	$0.021\,63 \pm 0.000\,30$	$0.022\,44 \pm 0.000\,19$	$0.022\,42 \pm 0.000\,18$	$0.022\,43 \pm 0.000\,18$
$\Omega_c h^2$	0.1148 ± 0.0034	$0.1184^{+0.0021}_{-0.0018}$	0.1188 ± 0.0012	0.1187 ± 0.0011
θ_{MC}	$0.010\,4249 \pm 0.000\,0071$	$0.010\,4185 \pm 0.000\,0063$	$0.010\,4179 \pm 0.000\,0060$	$0.010\,4180 \pm 0.000\,0059$
τ	0.0650 ± 0.0015	0.0649 ± 0.0015	0.0650 ± 0.0015	0.0650 ± 0.0015
$\log(10^{10}A_s)$	3.045 ± 0.016	$3.0684^{+0.0068}_{-0.0060}$	3.0700 ± 0.0051	3.0697 ± 0.0051
n_s	1.012 ± 0.016	$0.9761^{+0.0047}_{-0.0052}$	0.9752 ± 0.0039	0.9755 ± 0.0039
E_{11}	<0.259	$0.01^{+0.34}_{-0.55}$	0.02 ± 0.27	0.02 ± 0.27
E_{22}	<1.85	$0.30^{+0.66}_{-1.5}$	$0.13^{+0.51}_{-0.74}$	$0.13^{+0.51}_{-0.75}$
H_0	69.2 ± 1.4	$68.30^{+0.76}_{-0.90}$	68.10 ± 0.48	68.15 ± 0.46
σ_8	$0.811^{+0.040}_{-0.058}$	$0.820^{+0.032}_{-0.036}$	0.823 ± 0.020	0.823 ± 0.020
$\mu_0 - 1$	$-0.02^{+0.29}_{-0.60}$	$0.00^{+0.24}_{-0.38}$	0.01 ± 0.18	0.02 ± 0.19
$\eta_0 - 1$	$0.77^{+0.70}_{-1.6}$	$0.21^{+0.49}_{-0.96}$	$0.09^{+0.35}_{-0.51}$	$0.09^{+0.35}_{-0.52}$
$\Sigma_0 - 1$	0.12 ± 0.19	$0.008^{+0.077}_{-0.089}$	0.020 ± 0.070	0.021 ± 0.068

have large error bars, but are competitive with those obtained by the Planck collaboration (Planck Collaboration VI 2020a). Thus, this allows a wide variety of models within these bounds. Then, we include *WMAP* data in a joint analysis of ACT DR4 + *WMAP*. In this case, we note a slight improvement, of about a factor of 2, in the observational constraint on Σ, passing from ACT DR4 to ACT DR4 + *WMAP*. However, the other parameters do not show significant improvements. Additionally, we incorporate the SDSS and SN samples, which minimally improve the parametric space of the model. Notably, the inclusion of ACT DR4 + *WMAP* + SDSS and ACT DR4 + *WMAP* + SDSS + SN data does not yield statistically discernible differences in the analysis. In Table 2, we report the summary of the statistical analyses of the main parameters of interest considering ACT DR4 and its combinations with *WMAP*, SDSS, and SN. In Table 3, we report the results for the same data combination but now consider also the ACT DR6 lensing data. As expected, the presence of the CMB lensing improves the measurements on the light deflection parameter Σ_0. For the joint analysis, ACT DR4 + ACT DR6 lensing + *WMAP* + SDSS + SN, we find $\Sigma_0 - 1 = 0.021 \pm 0.068$ at 68 per cent confidence level (CL), which is stronger than the constraint obtained by the Planck collaboration (Planck Collaboration VI 2020a) that has $\Sigma_0 - 1 = 0.106 \pm 0.086$ at 68 per cent CL for *Planck* (including lensing) + SDSS + SN data. We notice here that the slight divergence from GR present for *Planck*, and due to the A_{lens} problem, is completely absent for the ACT data, for which GR is recovered within 1σ. This can clearly be seen in Fig. 1, which shows the one- and two-dimensional (68 and 95 per cent CL) marginalized distributions for MG parameters from the ACT DR4 data set alone and when combined with *WMAP*, SDSS, and SN.

Now, we adopt as a baseline in our analysis the SPT-3G data. In Table 4, we report the summary of the statistical analyses of the main parameters of interest considering SPT-3G individually and in combinations with *WMAP*, SDSS, and SN. Similar to the observations made in the ACT analysis, when we take SPT-3G into consideration, we find that all results remain consistent with the predictions of GR within 2σ. First, we note that SPT-3G only is slightly better when compared with ACT only (both cases with and without lensing). However, from a statistical perspective, even with these improvements, the parameters of interest still have large error bars, i.e. μ_0, η_0, and Σ_0. Moreover, SPT-3G only shows a slight indication at 1σ for deviations from GR. As a second step, we proceeded to combine SPT-3G with *WMAP*, SDSS, and SN. It is interesting to note that the joint analyses SPT-3G + *WMAP*, SPT-3G + *WMAP* + SDSS, and SPT-3G + *WMAP* + SDSS + SN yield nearly identical levels of accuracy as their corresponding counterparts involving ACT, and bring back the agreement with GR within the 68 per cent CL. We can see it in Fig. 2, which shows the one- and two-dimensional (68 and 95 per cent CL) marginalized distributions for MG parameters from the SPT-3G data set alone and in combination with *WMAP*, SDSS, and SN.

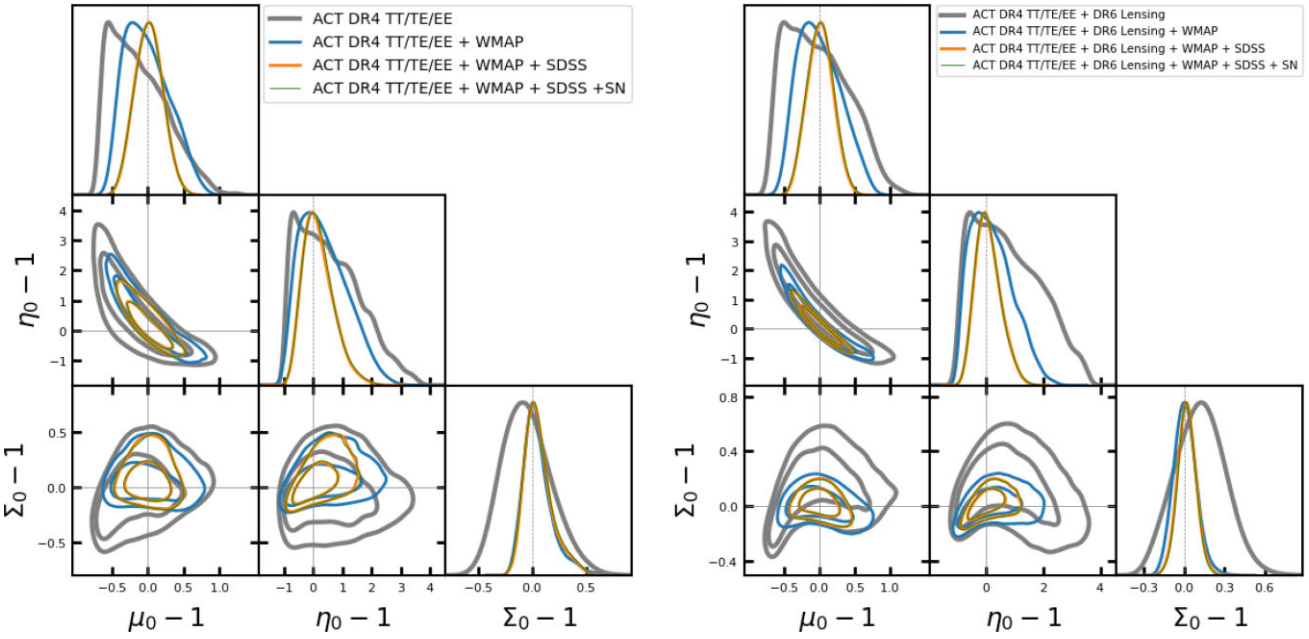

Figure 1. Left panel: Posterior distributions for MG parameters from the ACT DR4 data set alone and when combined with *WMAP*, SDSS (BAO + RSD), and SN. The 1σ and 2σ CLs are highlighted. Right panel: Same as in the left panel, but based on ACT DR4 + DR6 lensing data.

Table 4. Summary of 68 per cent CL limits for different data sets. SPT-3G = SPT-3G 2018 TT/TE/EE.

Parameter	SPT-3G	SPT-3G + *WMAP*	SPT-3G + *WMAP* + SDSS	SPT-3G + *WMAP* + SDSS + SN
$\Omega_b h^2$	$0.022\,17 \pm 0.000\,32$	$0.022\,42 \pm 0.000\,21$	$0.022\,39 \pm 0.000\,20$	$0.022\,39 \pm 0.000\,19$
$\Omega_c h^2$	0.1210 ± 0.0053	0.1161 ± 0.0028	0.1172 ± 0.0013	0.1172 ± 0.0013
θ_{MC}	$0.010\,3990 \pm 0.000\,0078$	$0.010\,4019 \pm 0.000\,0065$	$0.010\,4010 \pm 0.000\,0064$	$0.010\,4009 \pm 0.000\,0064$
τ	0.0650 ± 0.0015	0.0649 ± 0.0015	0.0649 ± 0.0015	0.0650 ± 0.0015
$\log(10^{10} A_s)$	3.073 ± 0.020	3.0546 ± 0.0093	3.0584 ± 0.0060	3.0583 ± 0.0060
n_s	0.960 ± 0.019	0.9696 ± 0.0067	0.9678 ± 0.0052	0.9682 ± 0.0052
E_{11}	<-0.289	$-0.03^{+0.34}_{-0.48}$	0.11 ± 0.26	0.10 ± 0.26
E_{22}	<0.434	$0.32^{+0.67}_{-1.4}$	$-0.14^{+0.44}_{-0.70}$	$-0.13^{+0.43}_{-0.72}$
H_0	$66.6^{+1.9}_{-2.2}$	68.6 ± 1.2	68.09 ± 0.53	68.11 ± 0.50
σ_8	0.794 ± 0.030	$0.800^{+0.029}_{-0.034}$	0.815 ± 0.019	0.815 ± 0.019
$\mu_0 - 1$	$-0.29^{+0.14}_{-0.35}$	$-0.02^{+0.24}_{-0.33}$	0.08 ± 0.18	0.07 ± 0.18
$\eta_0 - 1$	$0.03^{+0.38}_{-0.90}$	$0.23^{+0.56}_{-0.85}$	$-0.099^{+0.30}_{-0.49}$	$-0.09^{+0.30}_{-0.50}$
$\Sigma_0 - 1$	$-0.35^{+0.15}_{-0.22}$	$-0.003^{+0.077}_{-0.11}$	$-0.011^{+0.081}_{-0.10}$	$-0.009^{+0.078}_{-0.11}$

Comparing our results with those previously obtained in the literature is intriguing. For instance, Garcia-Quintero & Ishak (2021) investigated a similar parametrization using Planck 2018 data, both with and without lensing data. Their findings indicated $\mu_0 - 1 = 0.12^{+0.28}_{-0.54}$, $\eta_0 - 1 = 0.65^{+0.83}_{-1.3}$, and $\Sigma_0 - 1 = 0.29^{+0.15}_{-0.13}$ at 68 per cent CL, without lensing data. Comparatively, our analysis using ACT DR4, ACT, and SPT-3G data yielded constraints consistent with these findings, showcasing a similar level of accuracy as observed with *Planck* data alone. Furthermore, incorporating *WMAP*, SDSS, and SN samples into our analysis enhances the constraints beyond what is achieved relying solely on *Planck* data. In Lee et al. (2021), the MG functions μ, Σ, and η are constrained using cosmic shear data, with their combination with *Planck* data also explored. Our study's primary findings demonstrate competitive accuracy in constraining μ, Σ, and η, irrespective of the inclusion of *Planck* data.

5 CONCLUSION

From an observational point of view, it is widely established that the Universe is currently in a stage of accelerated expansion. In response, several modifications of GR have been proposed in the literature, aiming to offer a plausible mechanism for this accelerated expansion. Given the wide variety of models currently available in the literature that are capable of generating efficient modifications of GR, a practical approach placing observational constraints on deviations from GR is an interesting avenue. For instance, parametrizations that can encompass multiple classes of these models. In that regard, our analyses are conducted within the framework of the μ–Σ parametrization, where the μ–Σ parameters are responsible to captures such deviations.

We performed such analyses using alternative CMB data to the Planck dataset, which is known to be affected by the A_{lens} problem,

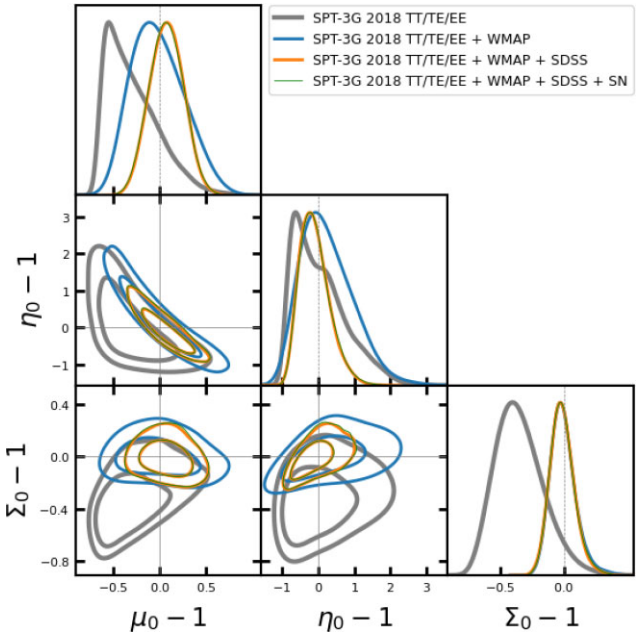

Figure 2. Posterior distributions for MG parameters from the SPT-3G data set alone and when combined with *WMAP*, SDSS (BAO + RSD), and SN.

biasing the results in favor of MG at 2σ level. The overarching goal is to derive novel observational constraints for these parameters, providing a fresh and unbiased perspective on their potential values. Using ACT and SPT data in combinations with SDSS (BAO + RSD) and SN samples, we have not found any deviations from the GR prediction. Our results represent an observational update on the well-known μ–Σ parametrization in view of all current CMB data. Notably, this update stands independent of the *Planck* data set, yet remains competitive with it. It is worth noting that discussions around *Planck* data within these frameworks have already been extensive.

In conclusion, while our current findings affirm the predictions of GR, it does not diminish the importance of continuing to explore MG theories. It might be possible that novel gravity parametrization models emerge as a compelling avenue for addressing the persistent anomalies and tensions within the ΛCDM framework, particularly those related to the H_0 and S_8 tensions. These discrepancies between predictions based on early Universe measurements and local Universe observations have prompted significant interest in understanding whether modifications to GR could provide a coherent explanation that bridges these gaps. Certainly, forthcoming precise measurements of CMB data hold the potential to shed light on MG frameworks, and potentially, it will be possible to provide evidence for any modifications of GR with CMB data, consequently reinforcing the significance of forthcoming CMB probes, including the CMB Stage IV mission (Abazajian et al. 2022).

ACKNOWLEDGEMENTS

The authors thank the referees for useful comments. It is also a pleasure to thank Gabriela Marques and Rodrigo von Marttens for their valuable assistance and support in completing this project. UA has been supported by the Department of Energy under contract DE-FG02-95ER40899, by the Leinweber Center for Theoretical Physics at the University of Michigan, and by Programa de Capacitação Institucional PCI/ON/MCTI during the initial stage of this project. AJSC thanks the financial support from the Conselho Nacional de Desenvolvimento Científico e Tecnologico for partial financial support under project no. 305881/2022-1, and the Fundação da Universidade Federal do Paraná (FUNPAR) by public notice 04/2023-Pesquisa/PRPPG/UFPR for partial financial support under process no. 23075.019406/2023-92. EDV was supported by a Royal Society Dorothy Hodgkin Research Fellowship. RCN thanks the financial support from the Conselho Nacional de Desenvolvimento Científico e Tecnologico for partial financial support under project no. 304306/2022-3, and the Fundação de Amparo à pesquisa do Estado do RS (FAPERGS) for partial financial support under project no. 23/2551-0000848-3. This article is based upon work from COST Action CA21136 addressing observational tensions in cosmology with systematics and fundamental physics (CosmoVerse) supported by COST (European Cooperation in Science and Technology). We also acknowledge the use of the High-Performance Data Center at the Observatório Nacional (CPDON) for providing the computational facilities to run our analyses.

DATA AVAILABILITY

All data used in this work are already publicly available.

REFERENCES

Abazajian K. N. et al., 2009, ApJS, 182, 543
Abazajian K. et al., 2022, preprint (arXiv:2203.08024)
Abbott T. M. C. et al., 2019, Phys. Rev. D, 99, 123505
Abbott T. M. C. et al., 2023a, Open J.Astrophys, 6, 2305
Abbott T. M. C. et al., 2023b, Phys. Rev. D, 107, 083504
Abdalla E. et al., 2022, J. High Energy Astrophys., 34, 49
Aiola S. et al., 2020, J. Cosmol. Astropart. Phys., 12, 047
Akrami Y. et al., 2021, preprint (arXiv:2105.12582)
Alam S. et al., 2017, MNRAS, 470, 2617
Alam S. et al., 2021, Phys. Rev. D, 103, 083533
Amon A. et al., 2022, Phys. Rev. D, 105, 023514
Andrade U., Anbajagane D., von Marttens R., Huterer D., Alcaniz J., 2021, J. Cosmol. Astropart. Phys., 11, 014
Asgari M. et al., 2021, A&A, 645, A104
Baker T., Bull P., 2015, ApJ, 811, 116
Baker T., Ferreira P. G., Leonard C. D., Motta M., 2014, Phys. Rev. D, 90, 124030
Balkenhol L. et al., 2023, Phys. Rev. D, 108, 023510
Bennett C. L. et al., 2013, ApJS, 208, 20
Beutler F. et al., 2012, MNRAS, 423, 3430
Blake C. et al., 2012, MNRAS, 425, 405
Brout D. et al., 2022, ApJ, 938, 110
Choi S. K. et al., 2020, J. Cosmol. Astropart. Phys., 12, 045
Dalal R. et al., 2023, preprint (arXiv: 2304.00701)
Davis M., Nusser A., Masters K. L., Springob C., Huchra J. P., Lemson G., 2011, MNRAS, 413, 2906
Deffayet C., Gao X., Steer D. A., Zahariade G., 2011, Phys. Rev. D, 84, 064039
Di Valentino E., Melchiorri A., Silk J., 2016a, Phys. Rev. D, 93, 023513
Di Valentino E. et al., 2021a, Class. Quantum Gravity, 38, 153001
Di Valentino E. et al., 2021b, Astropart. Phys., 131, 102604
dos Santos F. B. M., Gonzalez J. E., Silva R., 2022, Eur. Phys. J. C, 82, 823
Escamilla L. A., Giarè W., Di Valentino E., Nunes R. C., Vagnozzi S., 2023, preprint (arXiv:2307.14802)
Espejo J., Peirone S., Raveri M., Koyama K., Pogosian L., Silvestri A., 2019, Phys. Rev. D, 99, 023512
Frusciante N., 2021, Phys. Rev. D, 103, 044021
Garcia-Quintero C., Ishak M., 2021, MNRAS, 506, 1704
Giannantonio T., Martinelli M., Silvestri A., Melchiorri A., 2010, J. Cosmol. Astropart. Phys., 2010, 030
Heisenberg L., 2019, Phys. Rep., 796, 1

Horndeski G. W., 1974, Int. J. Theor. Phys., 10, 363
Huterer D., Shafer D. L., Scolnic D. M., Schmidt F., 2017, J. Cosmol. Astropart. Phys., 2017, 015
Ishak M., 2019, Living Rev. Rel., 22, 1
Jain B., Vikram V., Sakstein J., 2013, ApJ, 779, 39
Kase R., Tsujikawa S., 2019, Int. J. Mod. Phys. D, 28, 1942005
Kobayashi T., 2019, Rep. Prog. Phys., 82, 086901
Kumar S., Nunes R. C., Yadav P., 2023, Phys. Rev. D, 107, 063529
Lee S. et al., 2021, MNRAS, 509, 4982
Li X. et al., 2023, preprint (arXiv:2304.00702)
Lin M.-X., Raveri M., Hu W., 2019, Phys. Rev. D, 99, 043514
Madhavacheril M. S. et al., 2023, preprint (arXiv:2304.05203)
Moresco M., 2015, MNRAS, 450, L16
Nojiri S., Odintsov S. D., Oikonomou V. K., 2017, Phys. Rep., 692, 1
Nunes R. C., Vagnozzi S., 2021, MNRAS, 505, 5427
Nunes R. C., Pan S., Saridakis E. N., 2016, J. Cosmol. Astropart. Phys., 2016, 011
Padmanabhan T., 2003, Phys. Rep., 380, 235
Perivolaropoulos L., Skara F., 2022, New Astron. Rev., 95, 101659
Perlmutter S. et al., 1999, ApJ, 517, 565
Planck Collaboration XIV, 2016, A&A, 594, A14
Planck Collaboration VI, 2020a, A&A, 641, A6
Pogosian L., Silvestri A., Koyama K., Zhao G.-B., 2010, Phys. Rev. D, 81, 104023
Pogosian L. et al., 2022, preprint (arXiv:2107.12992)
Qu F. J. et al., 2023, preprint (arXiv:2304.05202)
Raveri M., Pogosian L., Martinelli M., Koyama K., Silvestri A., Zhao G.-B., 2023, J. Cosmol. Astropart. Phys., 2023, 061
Riess A. G. et al., 1998, AJ, 116, 1009
Riess A. G. et al., 2022, ApJ, 934, L7
Riess A. G. et al., 2023
Ross A. J., Samushia L., Howlett C., Percival W. J., Burden A., Manera M., 2015, MNRAS, 449, 835
Sakr Z., Martinelli M., 2022, J. Cosmol. Astropart. Phys., 2022, 030
Salvatelli V., Piazza F., Marinoni C., 2016, J. Cosmol. Astropart. Phys., 2016, 027
Sánchez A. G. et al., 2014, MNRAS, 440, 2692
Scolnic D. M. et al., 2018, ApJ, 859, 101
Song Y.-S., Percival W. J., 2009, J. Cosmol. Astropart. Phys., 2009, 004
Specogna E., Di Valentino E., Levi Said J., Nguyen N.-M., 2023, preprint (arXiv:2305.16865)
Srinivasan S., Thomas D. B., Pace F., Battye R., 2021, J. Cosmol. Astropart. Phys., 2021, 016
Taddei L., Martinelli M., Amendola L., 2016, J. Cosmol. Astropart. Phys., 2016, 032
Thomas D. B., 2020, Phys. Rev. D, 101, 123517
Tojeiro R. et al., 2012, MNRAS, 424, 2339
Torrado J., Lewis A., 2021, J. Cosmol. Astropart. Phys., 2021, 057
Velten H. E. S., vom Marttens R. F., Zimdahl W., 2014, Eur. Phys. J. C, 74, 3160
Wang Z., Mirpoorian S. H., Pogosian L., Silvestri A., Zhao G.-B., 2023, J. Cosmol. Astropart. Phys., 2023, 038
Weinberg S., 1989, Rev. Mod. Phys., 61, 1
Zarrouk P. et al., 2018, MNRAS, 477, 1639
Zhao G.-B., Pogosian L., Silvestri A., Zylberberg J., 2009, Phys. Rev. D, 79, 083513
Zhao G.-B., Giannantonio T., Pogosian L., Silvestri A., Bacon D. J., Koyama K., Nichol R. C., Song Y.-S., 2010, Phys. Rev. D, 81, 103510
Zlatev I., Wang L., Steinhardt P. J., 1999, Phys. Rev. Lett., 82, 896

This paper has been typeset from a TEX/LATEX file prepared by the author.